Article

Application of particle swarm optimization to understand the mechanism of action of allosteric inhibitors of the enzyme HSD17β13

Highlights

- Remove bias when interpreting mechanistic data for complex biological systems

- Characterize the oligomeric state of a protein dependent on inhibitor concentration

- Increase robustness for global analysis of thermal shift data

- Detect global minimum in the presence of several local minima

Authors

Amy Ford, Frauke Breitgoff, Miriam Pasquini, ..., Angeline Gavard, David Damerell, Martin Redhead

Correspondence

mredhead@exscientia.co.uk

In brief

Remove bias when interpreting mechanistic data for complex biological systems that characterize the oligomeric state of a protein dependent on inhibitor concentration. This method increases robustness for global analysis of thermal shift data with the potential to be applied to other data-rich biophysical techniques.

CellPress

Patterns

Article

Application of particle swarm optimization to understand the mechanism of action of allosteric inhibitors of the enzyme HSD17β13

Amy Ford,[1] Frauke Breitgoff,[1] Miriam Pasquini,[1] Amanda MacKenzie,[2] Stuart McElroy,[2] Steve Baker,[1] Patrizia Abrusci,[1] Simon Varzandeh,[1] Louise Bird,[1] Angeline Gavard,[1] David Damerell,[1] and Martin Redhead[1,3,*]

[1]Exscientia, The Schrödinger Building, Oxford Science Park, Oxford OX4 4GE, UK
[2]Bioascent, Bo'Ness Road, Chapelhall, Motherwell ML1 5SH, UK
[3]Lead contact
*Correspondence: mredhead@exscientia.co.uk
https://doi.org/10.1016/j.patter.2023.100733

THE BIGGER PICTURE Biological systems contain numerous components and points of regulation. These factors complicate mathematical modeling approaches; however, methods have been developed that explore the entire solution space before an optimal solution is selected. One such approach, particle swarm optimization, is based upon the swarming of birds. Each bird in the flock assesses multiple landing spots while at the same time sharing that information with its neighbors. Eventually, the entire flock chooses an optimal location based on food availability and the avoidance of predators. When transformed into multivariable equations, this behavior can remove bias when interpreting complex datasets. This can be a powerful tool in the pharmaceutical industry for the study of complex equilibria. Enhancements to these modeling approaches may allow for the analysis of higher-order kinetic and thermodynamic problems in biochemistry.

1 **2** 3 4 5   **Proof-of-Concept:** Data science output has been formulated, implemented, and tested for one domain/problem

---

SUMMARY

Understanding a drug candidate's mechanism of action is crucial for its further development. However, kinetic schemes are often complex and multi-parametric, especially for proteins in oligomerization equilibria. Here, we demonstrate the use of particle swarm optimization (PSO) as a method to select between different sets of parameters that are too far apart in the parameter space to be found by conventional approaches. PSO is based upon the swarming of birds: each bird in the flock assesses multiple landing spots while at the same time sharing that information with its neighbors. We applied this approach to the kinetics of HSD17β13 enzyme inhibitors, which displayed unusually large thermal shifts. Thermal shift data for HSD17β13 indicated that the inhibitor shifted the oligomerization equilibrium toward the dimeric state. Validation of the PSO approach was provided by experimental mass photometry data. These results encourage further exploration of multi-parameter optimization algorithms as tools in drug discovery.

INTRODUCTION

High-throughput screens (HTSs) are employed in drug discovery to identify enzyme inhibitors. Often, practitioners aim to find molecules that compete with the substrate of the enzyme; however, the possibility of false positives through undesirable pan-assay interference compounds (PAINs), as well as exotic allosteric mechanisms,[1,2] complicate interpretation. Biophysical techniques are employed as orthogonal methods to

confirm target engagement and to exclude undesirable mechanisms.[3] Compared with biochemical screens—which measure a single parameter of inhibition—biophysical techniques, such as thermal shift, are data rich and require specialized models to interpret.[4] A recent HTS revealed a micromolar inhibitor of HSD17β13. A fluorescent thermal shift assay was selected as orthogonal proof of binding, as this solution-based method would allow sampling of all oligomerization states of the protein. When the inhibitor was tested in a
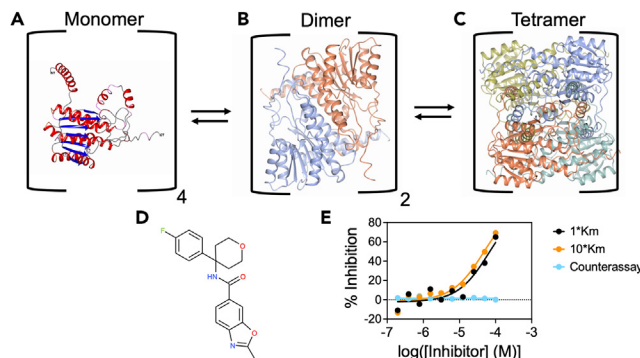
Figure 1. Kinetic scheme of HSD17β13 and the activity of the inhibitor

The protein exists in an equilibrium containing 3 species: a monomer (A), homodimer (B), and homotetramer (C). The chemical structure of the inhibitor is shown in (D). Enzymatic activity was measured in 384-well optiplates. Final concentration of HSD17β13 was 30 nM. Inhibitor was titrated and luminescence was monitored at room temperature for 60 min using a multimode plate reader (E). A counter assay was performed as described above except in the absence of HSD17β13 and quantified at 30 min.

thermal shift screen, it gave a shift of 15°C. The magnitude of this shift was unusually large given the micromolar potency[3–5]; thus, we hypothesized that the inhibitor was affecting oligomerization of the protein.

One of the most commonly used methods to measure drug candidate binding to proteins of therapeutic interest is the fluorescent thermal shift assay (FTSA).[6,7] FTSA has several advantages over other techniques, including ease of development, low reagent quantities and associated cost, and ability to be performed on standard thermal cycler instruments. The method is based on the observation that ligands alter protein thermal stability upon binding to the native state of the protein. This premise of FTSA has been expanded to include models assessing ligand binding to unfolded proteins and incorporation of techniques such as surface plasmon resonance to enhance the determination of biophysical parameters (e.g., K_D, k_{on}, k_{off}, ΔG, ΔS, and ΔH).[3] Despite its widespread application in the pharmaceutical industry, FTSA is limited by its largely qualitative metric, using only the change in protein melting temperature (ΔT_m). More quantitative methods have been described[8] wherein the thermodynamics and kinetics of ligand-induced stabilization have been investigated to generate models that describe thermal shift based upon the entropy of protein melting.[4] Thus, FTSA yields a data-rich output suitable for fitting complex biological systems.

Many cellular functions are carried out by large, multi-protein complexes.[9] Inherent to the formation of these complexes are numerous intermediate structures that exist in equilibrium. The hydroxysteroid dehydrogenases (HSDs), in their active form, may exist as both homodimers and tetramers stabilized by NADH.[10] Similarly, HSD17β13 dimerizes via binding events between αE and αF helices, interactions that are necessary for enzymatic activity.[10] Small-molecule inhibitors of these and other oligomeric enzymes may attribute their activity to shifts in the oligomerization equilibrium, a mechanism that may be derived via analysis of FTSA data. Thus, we hypothesized that

a potential reason for a compound with a weak μM IC50 causing a 15° thermal shift may be due to the inhibitor influencing the oligomerization of the HSD17β13 protein.

A model was developed to define the melting parameters of HSD17β13 in terms of monomer, dimer, and tetramer equilibrium. However, the requirement to simulate multiple reactions increased the complexity of the model and raised the number of unconstrained kinetic parameters.[11,12] Determining an optimum parameter dimensionality, therefore, may increase the robustness of the model and improve its predictive power, particularly when available experimental data are limited. A commonly used process for optimizing fitting of datasets in these settings is the Levenberg-Marquardt algorithm, which has demonstrated its performance in manifold applications such as communication systems, signal processing, and image analysis.[13,14] Non-convex problems—which can involve multiple local minima—require global optimization approaches to determine the global optimum, and approaches that do not require the objective function to be differentiable often greatly increase the speed of convergence.

A concept for the optimization of non-linear functions—termed particle swarm optimization (PSO)—was originally described by Kennedy and Eberhart in 1995.[12] In PSO, a number of particles are placed in the search space of a problem, and each evaluates the objective function at its location. Each particle then moves through the search space by combining aspects of the history of its own current and best locations with those of other members of the swarm. Successive iterations occur after all particles have been moved. Eventually, the swarm, like a flock of birds foraging for food, convenes at or near the global optimum of the fitness function.

PSO has several advantages over classic optimization techniques like linear gradient descent and quasi-Newton methods: (1) it makes few or no assumptions about the problem itself (i.e., it is metaheuristic), (2) it searches large spaces of candidate solutions, (3) it does not require the problem to be differentiable, and (4) it is flexible, easy to implement, and efficient. For finding an optimal set of hyper-parameters, naive methods such as grid and random search have been employed, which run large numbers of independent experiments under different hyper-parameter guesses and then select the best set. Contemporary versions of PSO have included different choices of hyper-parameters, different topologies, and varying ways of updating the hyper-parameters to improve its performance.[15] In software packages like *hydro*PSO,[16] for example, adjustments to—among other variables—particle size and acceleration coefficients can be made to achieve better performance than with the standard implementation. Despite these improvements, PSO has been shown to be vulnerable to sub-optimal solutions and premature convergence.[12] The use of PSO for optimization of the kinetics of chemical reactions has been explored and compared with the performance of using a genetic algorithm; PSO was found to perform better.[15]

Herein, we describe an approach using PSO alongside linear gradient decent to examine the effects of a small-molecule inhibitor of HSD17β13 on the enzyme's oligomerization equilibrium. Thermal shift data in the absence and presence of inhibitor were analyzed, and the best fitting parameters indicated that the inhibitor shifted the protein to the dimeric state. Validation
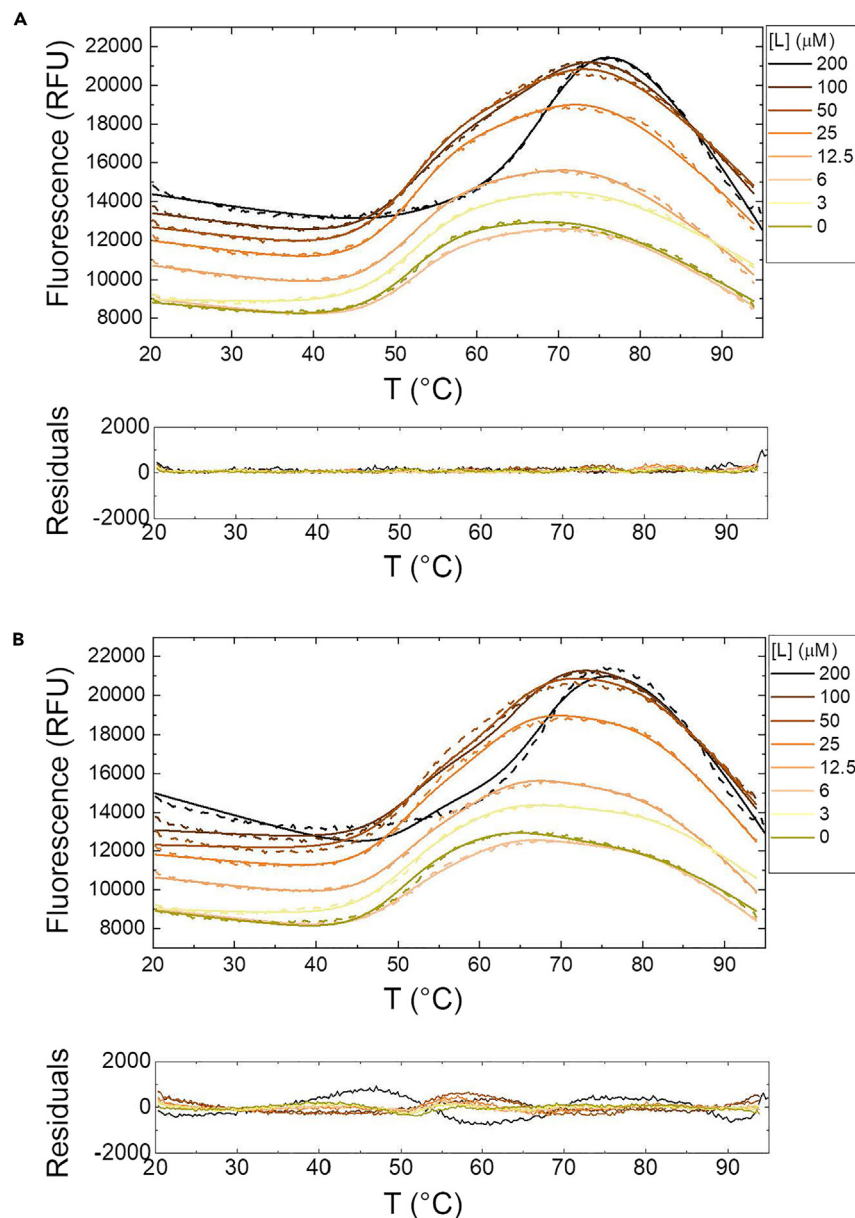
Figure 2. FTSA data from HSD17β13 alone and in the presence of varying concentrations of inhibitor

(A, top panel) The best individual fit (solid lines) of the raw fluorescence data (dashed lines) using PSO and linear gradient descent; bottom panel displays the residuals after fitting.

(B, top panel) Raw fluorescence data (dashed lines) as shown in (A). Repeated optimization of global and local parameters using PSO uncovered a second minima further refined using linear gradient descent (solid lines); the bottom panel displays the residuals after fitting. Parameter optimization using PSO and refinement via linear gradient descent were performed as outlined in the experimental procedures (see flowchart).

15° thermal shift was observed (Figure 2), which, for a simple single-site binding model, would imply an affinity in the low nM range.[3,4]

FTSA data with HSD17β13 alone and in the presence of increasing concentrations of inhibitor are presented in Figure 2. The best individual fit of the raw fluorescence data using PSO and linear gradient descent is shown in Figure 2A (top panel). Depending on the results' choice of the initial PSO steps, a fitting approach using PSO and linear gradient descent resulted in the closest global minimum (i.e., a set of parameters for which the sum of residuals was low; Figure 2A, bottom panel). However, repeated optimization of global and local parameters using the same fitting approach uncovered a second set of parameters (a second minimum) that could be further refined using linear gradient descent but resulted in higher residual levels (Figure 2B, top panel, and residuals, bottom panel). The results of the fit to the data in Figure 2A (detailed in Table 1) suggest that, in the presence of the inhibitor, the equilibrium of HSD17β13 is shifted to the dimeric state.

The fit parameters *beta* and *gamma* represent allosteric constants that describe the change in affinity for the equilibrium constants for dimerization and tetramerization upon inhibitor binding, respectively. The fitted value for *beta* is close to 1, indicating that dimerization is unaffected; however, *gamma* is very large (10^9), indicating a decrease in the affinity of tetramerization of several orders of magnitude (Table 1). This result indicates that the inhibitor would not bind to tetrameric protein and, equally, that the protein would not tetramerize with the inhibitor bound.

The affinity of the inhibitor binding to monomeric protein is given by *pKi* and calculated to be 1 mM. When *pKi* is converted via the allosteric constant of dimerization, 0.03 *alpha*, results in an affinity of the inhibitor to the dimeric form of 30 μM, which is in good agreement with the IC50 displayed in Figure 1. These

of these findings was provided by mass photometry data, demonstrating that increasing concentrations of the inhibitor progressively shifted the equilibrium away from the quaternary complex. Our approach using PSO can help to interpret complex protein kinetics without prior knowledge of the underlying biophysical parameters.

RESULTS

The experimental system used as a basis for PSO is shown in Figure 1. HSD17β13 exists in an equilibrium comprising monomeric (Figure 1A), dimeric (Figure 1B), and tetrameric (Figure 1C) states. This kinetic scheme was employed to define the PSO parameters. The IC50 of the inhibitor (Figure 1D) was determined in a cell-free assay (Figure 1E). Despite the IC50 of the inhibitor being in the μM range, a

Table 1. Fitting parameters and values derived from PSO and linear gradient descent (LGD)

	PARAMETERS								
	pKD1	dH1	dS1	dS2_factor	dS3_factor	logalpha	pKi	logbeta	loggamma
PSO	5.9	540,000	1,700	38	60	−0.5	3	−0.2	12
After LGD	4.7	230,000	710	27	9	−2.8	3	−0.2	8.7
SD (all LGD)	0.7	56,000	170	8	11	0.9	0.7	0.3	9.4
COV (%)	14	24	24	30	120	30	23	150	100

Parameters represent the following: pKD1, affinity of two monomers to form a dimer; dH1, enthalpy of melting; dS1, entropy of the first transition; dS2_factor, change in entropy of the second transition relative to the first transition; dS3_factor, change in entropy of the third transition relative to the first and second transitions; logalpha, the base 10 logarithm of the allosteric constant of dimerization; pKi, binding affinity of the inhibitor to monomeric protein; logbeta, the base 10 logarithm of the allosteric constant describing the change in affinity for the equilibrium constants for dimerization upon inhibitor binding; loggamma, the base 10 logarithm of the allosteric constant describing the change in affinity for the equilibrium constants for tetramerization upon inhibitor binding. SD and COV denote standard deviation and coefficient of variation, respectively.

results indicate that the inhibitor preferentially binds to and stabilizes the dimeric form of the protein.

The results of the fit were reproducible, with the coefficient of variation generally less than 30% (Table 1), except for *dS3_factor*—which describes the midpoint of the third transition—and *gamma*—which was so large as to be unreliable.

Figure 3 displays mass photometry data for HSD17β13 in the absence and presence of inhibitor. In the absence of the inhibitor, two peaks were observed in the range of 50 and 70 kDa and a third peak of lower intensity in the range of 130 kDa. The molecular weight of monomeric HSD17β13 is approximately 29 kDa. We tentatively assign the three peaks to the monomer, dimer, and tetramer species, respectively. In the presence of the inhibitor, the distribution was dominated by the peak corresponding to the dimer, suggesting that the inhibitor shifted the protein oligomerization equilibrium toward the dimeric state. These experimental results are consistent with the conclusions derived from the PSO and linear gradient descent approach to fitting the FTSA data.

DISCUSSION

PSO was initially described in 1995 and has been applied to interpret geological anomalies[17] and other non-biological activities. We have applied the methodology to data generated by FTSA to provide a quantitative description of a compound altering the multimerization equilibrium of a protein.

Unlike *in vitro* biochemical screens that are commonly used for HTS and that measure a single parameter (e.g., IC50), biophysical techniques like FTSA are data rich and require specialized computational methods to interpret. Such methods are also critical for investigating outliers in drug discovery campaigns, such as false positives. Here, we observed a surprising result, namely that a weak inhibitor of HSD17β13 produced a thermal shift that is consistent with a more potent compound. Thus, we employed PSO to explore the entire solution space to delineate the mechanism of inhibition.

The advantage of PSO is that, when applied to the entire solution space, an unbiased search of parameter space is performed, allowing for the identification of the best global parameters and neighboring local minima that, in this study, were refined using linear gradient descent (Figure 2; for more details regarding the fitting approach using PSO, see Figure 4). Despite this capability, PSO requires fine-tuning of

hyper-parameters like the personal and social acceleration coefficients (c_1 and c_2, respectively), number of particles, etc. Furthermore, repetition of PSO runs is needed, as we experienced an inherent failure rate (identification of a local instead of the global minimum) of 85%. However, in this case involving inhibitor-induced shifts in HSD17β13 equilibrium, the fits that led to the lowest residuals after the linear gradient descent refinement step consistently described the dimer as the dominant species in the presence of the inhibitor. Reducing failure rate would require more extensive fine-tuning of the hype-parameters, such as incorporating a greater number of informants and exploiting more random topologies. Mass photometry data (Figure 3) were found to be consistent with the inhibitor shifting the oligomerization equilibrium toward the dimeric state.

This method allows an unbiased approach using non-linear fitting to establish the mechanism of an inhibitor across a complex kinetic scheme. Previous methods[4] employed liner gradient descent that required the user to submit "best guess" starting parameters, which may introduce bias from the user as to where they think the solution should lie. Other methods define the starting parameters using features of the data, such as fluorescence values or graidents of cuvres; however, this this may also start the fit too close to a false minima to escape and discover the true minima if linear graident decent is used. This approach relies on the availability of a kinetic model where multiple mechanisms may be explained by the use of allosteric parameters; it is not suitable for models that describe a single type of kinetic behavior. Equally, although this method allows an increase in the complexity of the model compared with methods employing solely linear gradient, the method does not allow for an infinite level of complexity. Users should be careful to match high-parameter stochastic fitting methods to techniques that collect a high volume of data, as well as that have many independent conditions (i.e. concentrations) collected and analyzed together.

Despite these limitations, PSO, as described herein, accurately modeled the effects of inhibitor on HSD17β13 equilibrium in the absence of prior knowledge of the mechanism of action and without the intrinsic bias of linear gradient descent, in that PSO does not require "starting" parameters, which may influence the solution space searched. Moreover, these findings were derived from FTSA, which does not require specialized equipment like mass photometry. These results suggest that a fitting routing using PSO may be an unbiased approach that could be
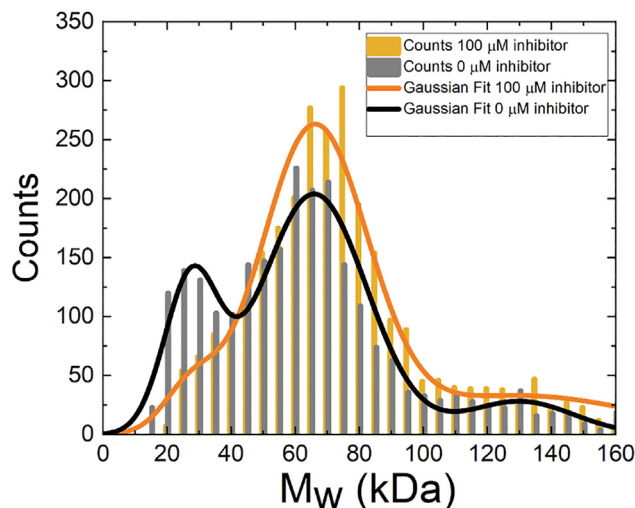
Figure 3. Mass photometry data for HSD17β13 in the presence and absence of inhibitor, shown as probability as a function of mass (bars) with a sum of three gaussians fitted to the data (lines)
In the absence of inhibitor, two peaks were observed in the range of 30 and 70 kDa and a third peak of lower intensity in the range of 130 kDa. We tentatively assign these to represent the monomer, dimer, and tetramer, respectively. The inhibitor increased the peak at 70 kDa, suggesting that the inhibitor shifted the equilibrium toward the dimeric state.

Figure 4. Flowchart demonstrating the process for generating and optimizing parameters using PSO and linear gradient descent
Fluorescence data for a "zero trace" (i.e., protein alone, no inhibitor) were measured and parameters were optimized using PSO and refined using linear gradient descent. PSO was then used to estimate local parameters on traces produced by increasing concentrations of inhibitor. Global parameters were then optimized using the PSO followed refinement of all parameters using linear gradient descent. The plots show representative fits after optimization by PSO (top) and after refinement by linear gradient descent (bottom).

implemented in other drug discovery campaigns to enable compound optimization regardless of therapeutic modality.

Conclusions

Determining a drug candidate's mechanism of action facilitates optimization of potency, physicochemical characteristics, and pharmacology. However, molecular targets often exist in equilibria with multiple higher-order structural states. Herein, we have shown that a combination of PSO and linear gradient descent—when applied to data derived from an extensively used fluorescence assay—models an inhibitor-induced equilibrium shift for HSD17β13, as confirmed by mass photometry. Thus, PSO may be broadly applicable to biological processes and enable an understanding of pathological and pharmacological perturbations.

EXPERIMENTAL PROCEDURES

Resource availability
Lead contact
Further information and requests for resources and reagents should be directed to and will be fulfilled by Martin Redhead (mredhead@exscientia.co.uk).
Materials availability
All unique/stable reagents generated in this study are available upon reasonable request to the lead contact.
Data and code availability
Our source code is available at GitHub (https://github.com/Exscientia/particle_swarm_ftsa) and datasets have been archived at Zenodo.[22]

Protein production
A PCR product with 15 bp vector-specific overhangs comprising amino acids 26–275 and utilizing the native DNA coding sequence of human HSD17β13 sequence (accession NM_178135) was cloned using In-Fusion (Takara,
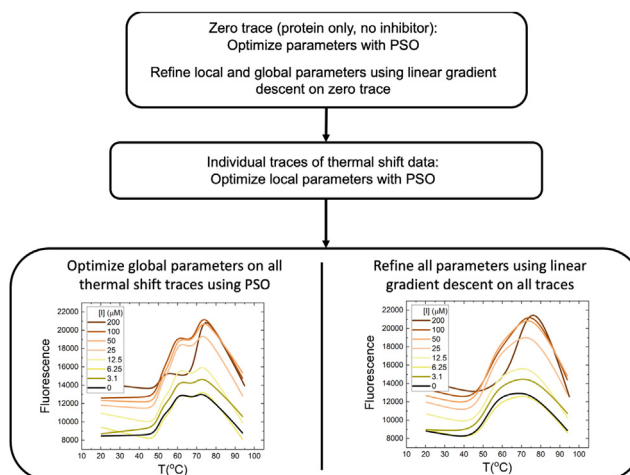
63969) into NcoI KpnI restricted pEXS2 to generate HSD17β13 26-275 with an N-terminal methionine and C-terminal 10-His affinity tag. The plasmid was transformed into Rosetta2 (DE3) cells (Sigma, 71400) and grown in Power Broth liquid media (Molecular Dimensions, MD12-117) at 37°C and 180 RPM to an OD600 between 0.6 and 0.8 before induction with a final concentration of 0.2 mM IPTG and continued to grow at 20°C for 20 h. HSD17β13 was purified in a two-step process: first, a Ni-NTA IMAC affinity purification, and second, a size-exclusion chromatography step on an ÄKTA Pure 25 system. Pools separating oligomeric states were in 20 mM HEPES (pH 7.5), 250 mM NaCl, and 1% glycerol and were flash frozen in liquid nitrogen before storing at −80°C. For a detailed purification protocol, please see the supplemental information.

Enzymatic assays
HSD17β13 activity was assayed in 384-well optiplates (PerkinElmer) in glycinamide assay buffer (20 mM glycinamide, 150 mM NaCl, 0.05% (v/v) Tween 20, 0.1 mg/mL BSA). Enzyme (4 μL; 30 nM) was pre-incubated with test compound for 15 min before the reaction was started by addition of NAD substrate (200 μM) and NADPH Glo reagent (Promega; 12 μL). Luminescence was monitored at room temperature for 60 min using a Pherastar FSX (BMG) multimode plate reader.

Counter-assay method
To assess the interaction between screen compounds and the detection reagent, a counter assay was run in the absence of HSD17β13. Compounds were incubated for 15 min in the presence of NADPH Glo reagent (Promega; 12 μL), followed by application of NADH substrate (720 nM; 4 μL) in glycinamide assay buffer. The reaction was quantified at 30 min using a Pherastar FSX (BMG) multi-mode plate reader.

FTSA and spectral fitting
The PySwarms package was employed to provide the PSO fitting[18], FTSA was conducted as described previously.[19] Briefly, HSD17β13 was incubated in the absence and presence of the inhibitor at increasing concentrations (0–200 μM). Fluorescence data for a "zero trace" (i.e., protein alone, no inhibitor) were generated and parameters were optimized using PSO. The model used is

described in the supplemental information. Linear gradient descent was performed on the "zero trace" following PSO to refine local and global fitting parameters, and the boundaries for the PSO were broad and based on physically realistic space (positive melting enthalpies, binding constants >0). PSO was used on the individual traces (i.e., each inhibitor concentration) of thermal shift data to optimize local parameters, which subsequently were refined with linear gradient descent. Then, optimal global parameters for all traces were determined using PSO and refined using linear gradient descent.[18] An outline of this general approach is shown in the flowchart displayed in Figure 4, with each box representing a step in the data fitting process.

Mass photometry

The purified protein was concentrated to 1.7 mg/mL and, prior to the MP measurement, pre-incubated with buffer (20 mM glycinamide, 150 mM NaCl, 5% DMSO) for 2 h. Each MP measurement was performed on glass coverslips and recorded using a OneMP mass photometer, Refeyn, for an interval of 60 s. Sample stocks at 100 nM were diluted in the appropriate buffer on glass coverslips to 10–50 nM. One of the samples contained solely protein in buffer, while 200 μM compound 1 was added to the other sample. Image processing was performed with the software DiscoverMP (Refeyn, v.2.4.2) as described.[20,21] After background removal, molecular weights of particles were estimated by contrast comparison with calibrants of known mass measured on the same day. Figure 3 shows the probability density function of counts of particles per mass as histograms with a bin width of 2.8 kDa.

SUPPLEMENTAL INFORMATION

Supplemental information can be found online at https://doi.org/10.1016/j.patter.2023.100733.

AUTHOR CONTRIBUTIONS

A.F., F.B., and S.B. wrote the PSO software and contributed to the manuscript development. M.P. performed the FTSA experiments. A.M. and S.M. performed the enzyme assays. P.A. and S.V. produced the protein and performed the mass photometry experiments. D.D. and M.R. conceptualized the study, provided oversight, and contributed to the manuscript development.

DECLARATION OF INTERESTS

A.F., F.B., S.B., M.P., P.A., S.V., L.B., D.D., and M.R. are employees and shareholders of Exscientia plc but declare no further conflict of interest.

REFERENCES

1. Screening for Allosteric Kinase Inhibitors in High Throughput - 2010 - Wiley Analytical Science https://analyticalscience.wiley.com/do/10.1002/gitlab.708.

2. Simard, J.R., Grütter, C., Pawar, V., Aust, B., Wolf, A., Rabiller, M., Wulfert, S., Robubi, A., Klüter, S., Ottmann, C., and Rauh, D. (2009). High-throughput screening to identify inhibitors which stabilize inactive kinase conformations in p38α. J. Am. Chem. Soc. *131*, 18478–18488.

3. Redhead, M., Satchell, R., Morkūnaitė, V., Swift, D., Petrauskas, V., Golding, E., Onions, S., Matulis, D., and Unitt, J. (2015). A combinatorial biophysical approach; FTSA and SPR for identifying small molecule ligands and PAINs. Anal. Biochem. *479*, 63–73.

4. Redhead, M., Satchell, R., McCarthy, C., Pollack, S., and Unitt, J. (2017). Thermal shift as an entropy-driven effect. Biochemistry *56*, 6187–6199.

5. Zubrienė, A., Matulienė, J., Baranauskienė, L., Jachno, J., Torresan, J., Michailovienė, V., Cimmperman, P., and Matulis, D. (2009). Measurement of nanomolar dissociation constants by titration calorimetry and thermal shift assay – radicicol binding to Hsp90 and ethoxzolamide binding to CAII. Int. J. Mol. Sci. *10*, 2662–2680.

6. Lo, M.C., Aulabaugh, A., Jin, G., Cowling, R., Bard, J., Malamas, M., and Ellestad, G. (2004). Evaluation of fluorescence-based thermal shift assays for hit identification in drug discovery. Anal. Biochem. *332*, 153–159.

7. Pantoliano, M.W., Petrella, E.C., Kwasnoski, J.D., Lobanov, V.S., Myslik, J., Graf, E., Carver, T., Asel, E., Springer, B.A., Lane, P., and Salemme, F.R. (2001). High-density miniaturized thermal shift assays as a general strategy for drug discovery. J. Biomol. Screen *6*, 429–440.

8. Cimmperman, P., Baranauskiene, L., Jachimoviciūte, S., Jachno, J., Torresan, J., Michailoviene, V., Matuliene, J., Sereikaite, J., Bumelis, V., and Matulis, D. (2008). A quantitative model of thermal stabilization and destabilization of proteins by ligands. Biophys. J. *95*, 3222–3231.

9. Alberts, B. (1998). The cell as a collection of protein machines: preparing the next generation of molecular biologists. Cell *92*, 291–294.

10. Kristan, K., Deluca, D., Adamski, J., Stojan, J., and Rižner, T.L. (2005). Dimerization and enzymatic activity of fungal 17β-hydroxysteroid dehydrogenase from the short-chain dehydrogenase/reductase superfamily. BMC Biochem. *6*, 28.

11. Hafiz, A.R., Amin, M.F., and Murase, K. (2012). Using complex-valued Levenberg-Marquardt algorithm for learning and recognizing various hand gestures. In Proceedings of the International Joint Conference on Neural Networks.

12. Kennedy, J., and Eberhart, R. (1995). Particle swarm optimization. Proc. ICNN'95 - Int. Conf. Neural Networks *4*, 1942–1948.

13. Levenberg, K. (1944). A Method for the solution of certain non-linear problems in least squares. Q. Appl. Math. *2*, 164–168.

14. Marquardt, D.W. (1963). An algorithm for least-squares estimation of nonlinear parameters. J. Soc. Ind. Appl. Math. *11*, 431–441.

15. Poli, R., Kennedy, J., and Blackwell, T. (2007). Particle swarm optimization. Swarm Intell. *1*, 33–57.

16. Zambrano-Bigiarini, M., and Rojas, R. (2013). A model-independent particle swarm optimisation software for model calibration. Environ. Model. Softw. *43*, 5–25.

17. Essa, K.S., and Elhussein, M. (2018). PSO (particle swarm optimization) for interpretation of magnetic anomalies caused by simple geometrical structures. Pure Appl. Geophys. *175*, 3539–3553.

18. Miranda. (2018). PySwarms: a research toolkit for particle swarm optimization in. J. Open Source Softw. *3*, 433.

19. Kazlauskas, E., Petrauskas, V., Paketurytė, V., and Matulis, D. (2021). Standard operating procedure for fluorescent thermal shift assay (FTSA) for determination of protein–ligand binding and protein stability. Eur. Biophys. J. *50*, 373–379.

20. Sonn-Segev, A., Belacic, K., Bodrug, T., Young, G., VanderLinden, R.T., Schulman, B.A., Schimpf, J., Friedrich, T., Dip, P.V., Schwartz, T.U., et al. (2020). Quantifying the heterogeneity of macromolecular machines by mass photometry. Nat. Commun. *11*, 1772.

21. Olerinyova, A., Sonn-Segev, A., Gault, J., Eichmann, C., Schimpf, J., Kopf, A.H., Rudden, L.S.P., Ashkinadze, D., Bomba, R., Frey, L., et al. (2021). Mass photometry of membrane proteins. Chem *7*, 224–236.

22. Ford, A., Breitgoff, F., Pasquini, M., MacKenzie, A., McElroy, S., Baker, S., Abrusci, P., Varzandeh, S., Bird, L., Gavard, A., et al. (2023). Datasets for Application of particle swarm optimization to understand the mechanism of action of allosteric inhibitors of the enzyme HSD17ß13. https://doi.org/10.5281/zenodo.7744011.